our point of view, this conclusion that long-range order is not essential to sustain the cooperative intensity mechanism is of great importance. This is because we are interested in seeing whether the "long short-range order" along individual chains is sufficient to allow spin waves to exist above T_N. We see no spectral feature that can be directly associated with a magnon sideband (all of the optical experiments are at $>T_N$). Since the enhanced intensity can come from quite short-range order (only nearest neighbor?), and since the intensities show a smooth dependence on temperature in the region of χ_{max}, we interpret our results to mean that "long short-range order" along the chain is *not* particularly effective as far as the intensities are concerned. The question of the existence of spin waves above T_N is left open until other experiments bearing on this point are concluded.

ACKNOWLEDGMENTS

We thank L. R. Walker and R. L. Martin for several interesting discussions concerning this work. G. W. Hull, Jr., and R. C. Sherwood are thanked for obtaining some of the magnetic results.

PHYSICAL REVIEW VOLUME 187, NUMBER 2 10 NOVEMBER 1969

Nuclear Magnetic Relaxation of Domain-Wall Nuclear Spins via Magnon Interactions in Fe

MARY BETH STEARNS
Ford Scientific Laboratory, Dearborn, Michigan 48120
(Received 24 April 1969)

Measurements of the longitudinal and transverse relaxation rates of Fe^{57} nuclei in the domain walls of natural and enriched Fe have been made over the temperature range 1.2–295°K by use of spin-echo techniques. The relaxation times are found to vary with position in the wall as $T_0/\mathrm{sech}^2 x$, where x is the distance from the center of the wall (measured in wall-width units) and T_0 is the shortest relaxation time, at the center of the wall. In natural Fe, the relaxation rates vary linearly with temperature over the whole temperature range. This linear temperature variation and the shape of the relaxation curves give independent evidence that the main mode of both longitudinal and transverse relaxation in natural iron is via emission or absorption of single real-bulk magnons. For natural Fe, we find that $1/T_{01}T=22\pm2$ deg^{-1} sec^{-1} and $1/T_{02}T=28\pm3$ deg^{-1} sec^{-1}. At 1.2 and 4.2°K, we observe other relaxation mechanisms in a 90.7% enriched Fe^{57} sample. The dominant mechanism here is believed to be a spin-spin interaction of the Suhl-Nakamura type.

I. INTRODUCTION

PREVIOUS investigators have obtained a variety of values for both the nuclear longitudinal (T_1) and transverse (T_2) relaxation times of Fe^{57}. The longitudinal relaxation times obtained are listed in Table I. The interpretation of the spread in these values was attributed to a mixture of signals coming from the domains and domain walls.[1,2] We show here that this interpretation is incorrect and that for multidomain particles, the nuclear resonance signal is due mainly to nuclei in the domain walls where the nuclear spins are characterized as having different enhancement factors[3,4] and relaxation times depending upon their location in the domain wall. When this behavior is properly incorporated into the analysis we find independent evidence from *both* the temperature dependence and the shape of the relaxation curves to identify the mode of nuclear relaxation. In pure natural Fe (2.2% Fe^{57}) over the range 1.2–300°K, the main mode of both the longitudinal and transverse relaxation appears to be due to emission or absorption of single real-bulk magnons. For an enriched (90.7% Fe^{57}) Fe sample at 1.2 and 4.2°K we observed an additional transverse relaxation mechanism. This is thought to be due to a spin-spin interaction of the Suhl-Nakamura type. [Nuclear spin flips due to the emission (absorption) of a virtual magnon

TABLE I. Measured longitudinal relaxation time T_1 in msec.

Source	Temperature °K 4.2	78	295
a	20	~2	~1.5
b, c	10–500	0.7–11	0.9–6.5
d		1.3	0.25
e	600	32	8
f	11+1	0.55±0.05	0.16±0.03

[a] C. Robert and J. W. Winters, Compt. Rend. **250**, 3831 (1960).
[b] Reference 1.
[c] Reference 2.
[d] D. L. Cowan and L. W. Anderson, Phys. Rev. **135**, A1046 (1964).
[e] A. M. Portis and R. H. Lindquist, in *Magnetism IIA*, edited by G. T. Rado and H. Suhl (Academic Press Inc., New York, 1965), p. 357.
[f] Center of wall. M. B. Stearns, Phys. Letters **27A**, 706 (1968).

[1] M. Weger, E. L. Hahn, and A. M. Portis, J. Appl. Phys. **32**, 124S (1961).
[2] M. Weger, Ph.D. thesis, University of California, Berkeley, 1961 (unpublished); Phys. Rev. **128**, 1505 (1962).
[3] M. B. Stearns, Phys. Rev. **162**, 496 (1967).
[4] M. B. Stearns and A. W. Overhauser, J. Appl. Phys. **39**, 440 (1968).

TABLE II. Measured relaxation times and enhancement factors at the center of the wall for natural Fe samples.

Temp. (°K)	Sample 1[a] T_{01} (msec)	Sample 1[a] T_{02} (msec)	Sample 1[a] ϵ_0	Sample 2[b] T_{01} (msec)	Sample 2[b] ϵ_0
1.2	40±5	33±2	4100±200		
4.2	11±1	11±2	6100±300	10±1	~2000
15	3±0.5				
78	0.55±0.05	0.45±0.05	9500±500	0.42±0.05	~2500
295	0.16±0.03		25000±2000	0.14±0.03	~5500

[a] 99.999% Fe, Johnson-Matthey 1–10 μ needlelike.
[b] 99% Fe, General Anilene and Film Corporation 3–5 μ spheres.

by one nucleus and subsequent reabsorption (emission) by a second nucleus.]

II. EXPERIMENTAL PROCEDURE

The experimental apparatus is the same as that described by the author elsewhere.[3] The samples were polycrystalline multidomain powders of dimensions of a few microns. Two Fe samples with the natural Fe^{57} abundance were used. Sample 1 was 99.999% pure Fe from Johnson-Matthey. It was mainly needlelike in shape with the longest dimension varying from 1–10 μ. Sample 2 was 99.0% pure Fe, the other constituents were mainly C, N, and O. The particles of sample 2 had a spherical shape of 3–5 μ diam. However, they have an onionlike structure with layers of C, N, and O, between layers of Fe so that the demagnetizing factors of this material may not be that of a sphere. Although sample 2 has only 99.0% Fe, the segregrated nature of the sample evidently leads to Fe-rich regions of much higher nominal purity than 99.0%. The results were not particularily sensitive to size or shape of the particles, although perhaps the actual variation between samples was not sufficient to show such effects.

Measurements were also made on a 90.7% Fe^{57} enriched-Fe sample and some dilute-Fe alloys containing Al or Co. The enriched iron was obtained from Oak Ridge National Laboratory, Stable Isotope Division, and the results obtained with this sample indicate that it was quite impure. [Fe samples with an appreciable amount of disordered impurities have much shorter free induction decay (FID) times and much longer T_1 values than pure-Fe samples.]

All experiments were performed at the resonant frequency ~46 MHz. The longitudinal relaxation curves for the pure-Fe samples were obtained by measuring FID amplitude of the second of two rf pulses as a function of the time interval t between the pulses. For the alloys, the FID time is short (1–3 μsec), and thus the FID signal was obscured by the recovery time of the receiver. Therefore, the second pulse was replaced by a pair of pulses, and the longitudinal relaxation curves were obtained by measuring the height of the echo obtained from the pair of pulses as a function of the time t between the first pulse and the pair of pulses.

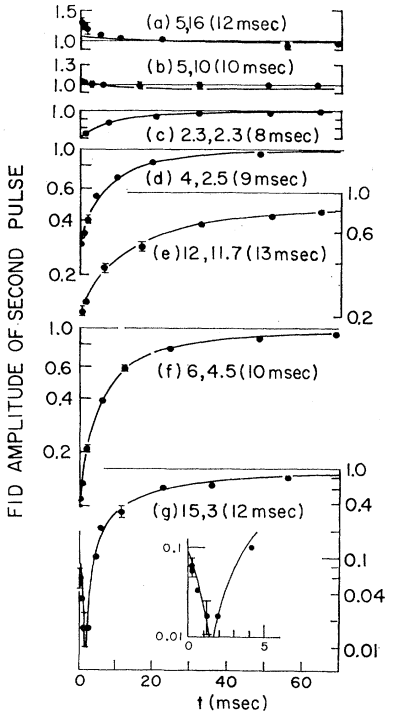

FIG. 1. Some typical relaxation curves of FID amplitude of the second of two pulses as a function of the time between pulses. The data points are for sample 2 at 4.2°K. The curves shown are calculated assuming $1/T_1(x)=\mathrm{sech}^2 x/T_{01}$ as would result from the emission or absorption of a single magnon. The numbers given near each curve give the maximum turning angles of the first and second pulses and the value of T_{01} used in the calculation. For example, curve (d) had maximum turning angles of $\alpha_1=4$ rad, $\alpha_2=2.5$ rad, and $T_{01}=9$ msec. Note the wide variety of decay curves obtained by varying the turning angles of the two pulses.

The time between the pair of pulses was fixed and always kept small compared to t and T_1. The time between each set of pulses was kept much larger than the longest relaxation time so that the spin system had returned to its equilibrium value for each measurement. The transverse relaxation time was measured in the usual way by measuring the echo height as a function of time between the two pulses generating the echo.

The usual procedure in making a relaxation time measurement was the following: First we measured the rf field B_1 in the sample. This was done by measuring the voltage developed across a single turn of wire fitting closely around the powdered sample; the samples were loosely packed in thin-walled Mylar cylinders. Next we measured the enhancement factor of the sample by measuring the FID amplitude of a single pulse or the echo height of a pair of pulses as a function of B_1 for a fixed pulse length (as described in Ref. 3). In this way we ascertained the turning angles for each of the pulses used in the relaxation-time measurements. Values obtained for the enhancement factors are listed in columns 4 and 6 of Table II. Notice that the enhancement factor increases with an increase in temperature. This is

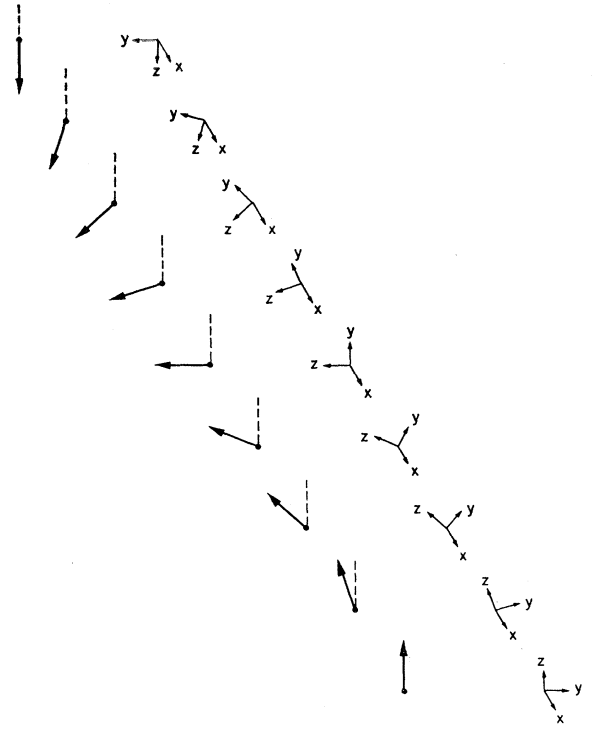

FIG. 2. Some representative spins through a 180° Bloch wall. Transposed laterally to the right are the coordinate systems in the rotating frame for each spin. A domain wall in Fe has a thickness of about 300 atomic layers.

believed to be due to an increase in the average drumhead radius with increasing temperature, as discussed in Ref. 3.

III. LONGITUDINAL RELAXATION TIMES IN PURE NATURAL Fe

A wide variety of shapes for the T_1 relaxation curves can be obtained depending upon the turning angle of the two pulses. Figure 1 shows some typical decay curves of the FID amplitude of the second pulse as a function of time between two pulses for various turning angles of the two pulses. We see the striking dependence of the relaxation curves on the turning angles. These shapes can be calculated using the previously obtained formulas (Refs. 3, 4) which properly represent the behavior of domain-wall nuclei. In Ref. 3 we showed that the domain-wall motion is well described by a drumhead model, where the wall is pictured as a circular membrane which oscillates like a drumhead in an rf field. We calculate the decay curves as follows: For each atom let the z direction be that of the electron spin and let the effective rf field at the nucleus be taken as the y direction in the rotating frame. z and y will vary across the wall as shown in Fig. 2. At resonance ($\omega=\omega_0$) the x component of the nuclear magnetization in the rotating frame (which is a measure of the FID) varies as $\sin(\gamma\epsilon B_1\tau)$, and the FID amplitude $\mathfrak{A}$ of a single pulse is given by

$$\mathfrak{A}(\omega_0,B_1,\tau)\sim\int_0^1\int_0^1\int_0^\infty\int_0^{\pi/2}\epsilon\sin(\gamma\epsilon B_1\tau)\times p(h)r\sin\eta d\eta dx dr dh, \quad (1)$$

where γ is the gyromagnetic ratio, B_1 is the rf field strength, τ is the pulse length, and η is the angle between B_1 and the magnetization on either side of the wall. (The wall oscillations cause the rf component parallel to the wall to be translated into an rf field in the y direction as defined above.) The enhancement factor of a particular nucleus at position (x,r) is $\epsilon=\epsilon_0(\mathrm{sech}x)\times(1-r^2)h\cos\eta$, where x is the perpendicular distance (in wall-width units) from the central plane of the wall, and r is the radial position of the nucleus. The factor $\mathrm{sech}x$ results from the rate of change of the electron-spin direction across a domain wall. The wall is regarded as a circular membrane with the radius of the membrane normalized to 1. The quantity h is the maximum displacement at the center of the membrane measured relative to the maximum displacement of the largest-area membrane. We have assumed that the probability distribution $p(h)$ of the h's is a constant. (See Ref. 3.) Thus, ϵ_0 is the maximum enhancement factor of a nucleus at the center of the wall.

Throughout this work we assume that the longitudinal and transverse components decay independently; that is, they are described by the Bloch equations $dM_z/dt=-(M_0-M_z)/T_1$ and $dM_{x,y}/dt=-M_{x,y}/T_2$. Now consider a pair of pulses separated by a time t. After the first pulse, the z component of a nuclear spin (initially taken as 1) is decreased by $(1-\cos\alpha_1)$, where $\alpha_i(=\gamma\epsilon B_1\tau_i)$ is the turning angle during the ith pulse. Let us assume that the z-component decrement relaxes exponentially as e^{-t/T_1}, so that at time t the z component is $1-(1-\cos\alpha_1)e^{-t/T_1}$. The second rf pulse then turns this z component through an angle $\alpha_2(=\gamma\epsilon B_1\tau_2)$ (the rf magnitude B_1 is kept the same for both pulses). Thus the FID amplitude of the second pulse $\mathfrak{A}_2$ is given by replacing $\sin\alpha_1$ in Eq. (1) with $\sin\alpha_2[1-(1-\cos\alpha_1)]e^{-t/T_1}$. Thus, we obtain

$$\mathfrak{A}_2(\omega_0,B_1,\tau_1,\tau_2)\sim\int_0^1\int_0^1\int_0^\infty\int_0^{\pi/2}\epsilon\sin\alpha_2\times[1-(1-\cos\alpha_1)]e^{-t/T_1}p(h)r\sin\eta d\eta dx dr dh. \quad (2)$$

We obtain the decay curves by evaluating Eq. (2) with a computer. It should be emphasized that the only unknown parameter in evaluating these curves is T_1; all the other parameters (ϵ_0, B_1, τ_1, and τ_2) are known from auxiliary measurements taken under the same conditions as used in measuring the relaxation curves.

If we assume T_1 is a constant throughout the wall, we find that Eq. (2) does *not* give satisfactory fits to the

data. This is demonstrated in Fig. 3, where the dashed curves are evaluated from Eq. (2) by use of the values of T_1 (in msec) shown labeling each curve. (The solid curve was calculated under the assumption that T_1 varies in a definite manner with position in the wall as discussed below.) As is seen in Fig. 3, we found that in order to get even mediocre fits to the data with T_1 constant across the wall we had to change T_1 quite drastically for the various operating conditions. For instance, the best fit for the data for curve (e), which had rather large turning angles, required $T_1=40$ msec, where the (f) data with smaller turning angles required a $T_1=18$ msec. Thus, considering only the variation-in-enhancement factor in the wall does not account satisfactorily for the behavior of the observed decay curves. We shall see below that for a physically reasonable variation of T_1 across the wall, decay curves taken under widely different combinations of turning angles can be fit with just one parameter.

We thus consider what further factors should be included in order to describe the relaxation process. Let us assume that in ferromagnetic materials the principal mechanism of nuclear relaxation is through interactions with real magnons. Furthermore, here we shall consider, for purposes of estimation, that the relaxation takes

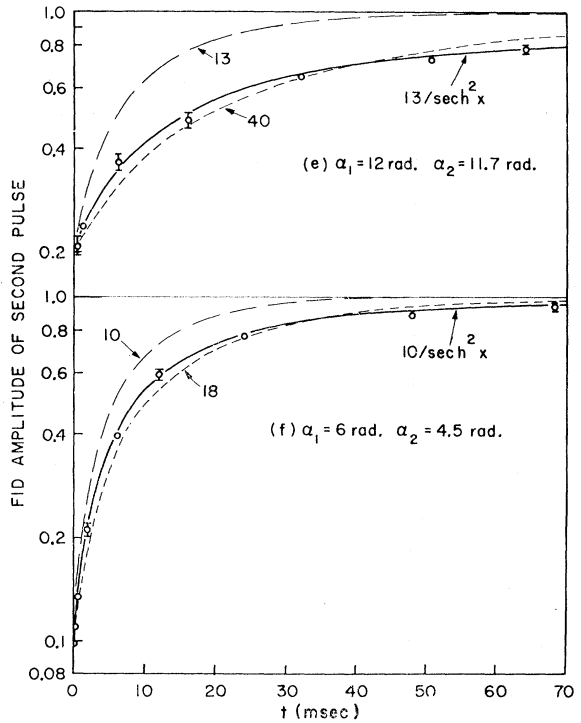

FIG. 3. Comparison of FID calculations from Eq. (2) with experimental data. The dashed curves are calculated assuming all nuclei have the same relaxation time T_1 independent of position in the wall; under this assumption curve (e) is fitted best, but not well, with $T_1=40$ msec, whereas curve (f) is best fit with $T_1=18$ msec. Far better agreement is obtained when it is assumed that $T_1=T_{01}/\mathrm{sech}^2 x$, as shown by the solid curves and discussed in the test.

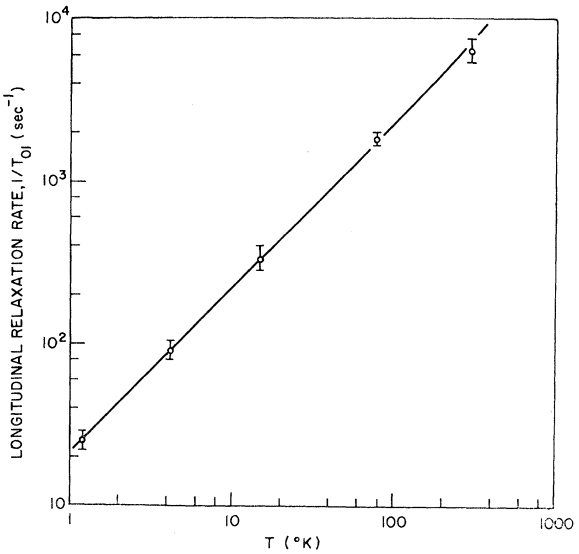

FIG. 4. Variation of the longitudinal relaxation rate at the center of the wall as a function of temperature. The solid line corresponds to $1/T_{01}T=22$ sec^{-1} deg^{-1}. This linear dependence gives evidence that the relaxation mechanism is via emission or absorption of single bulk magnons.

place through interaction with bulk magnons. We choose to consider bulk magnons rather than magnons due to wall-type excitations as discussed by Winter[5] for the following reasons: Because of the demagnetizing fields in ferromagnetic materials it is reasonable to expect that there are many bulk magnons with frequencies in the region of the nuclear-resonance frequency. The wall-type excitations have a frequency of $\sim$500 Mc/sec, and Winter found it necessary to artificially spread out the spectral density of these wall excitations by a random-force technique with a rather arbitrary width attributed to a damping parameter Γ. Since the parameter Γ would be temperature-dependent, Winter states that the "relaxation rate at the center of the wall does not vary with temperature as kT." This is at variance with the experimentally observed temperature dependence which, as seen from Figs. 4 and 6, does vary linearly with temperature over the whole temperature range 1.2–300°K. Indeed, this strictly linear variation indicates that the magnons causing the relaxation are *not* associated with wall-type excitations, since all wall parameters would be expected to be quite temperature-dependent and thus remove the simple linear dependence which arises from the magnon statistics. Winter found that the amplitude of his spin-wave-like excitations (which would correspond to bulk magnons) falls off inside the wall for the small k limit and therefore concluded that the "spin-wave-like solution is not very important for the relaxation in the wall." However, this type of calculation is very difficult and contains many

[5] J. M. Winter, Phys. Rev. **124**, 452 (1961). See also J. F. Janak, *ibid.* **134**, A411 (1964).

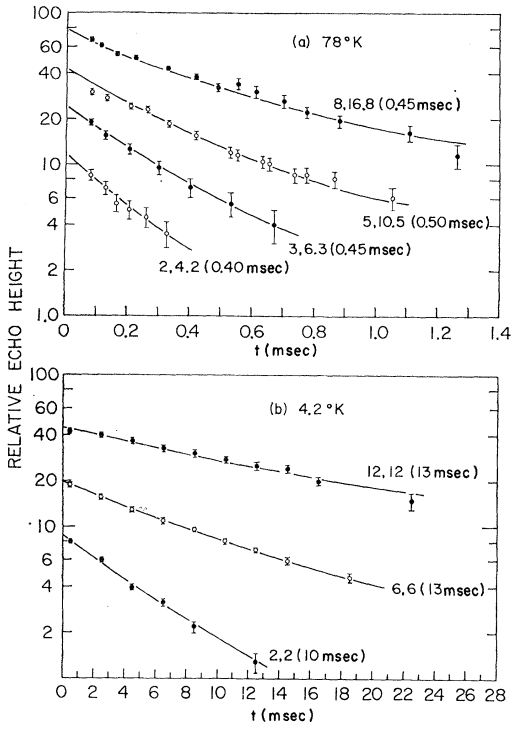

FIG. 5. Typical transverse relaxation curves of echo height as a function of the time between pulses for sample 1 at (a) 78°K and (b) 4.2°K. The curves are calculated assuming $1/T_2(x) = \text{sech}^2x/T_{02}$, as would result from emission or absorption of a single magnon. The numbers labeling each curve give the maximum turning angles of the two pulses and the value of T_{02} used in the calculation. The relative positions of the curves are not meaningful.

simplifying assumptions (e.g., small wave vector k, the demagnetizing terms used are only correct near the center of the wall, the functional form for the two spin directions in the wall is assumed to be same within a constant multiplier, etc.).

For these reasons, we assume the relaxation is due to bulk magnons. There will necessarily be some coupling between these magnons and the domain walls causing the latter to oscillate at the low bulk-magnon frequencies. This coupling of the magnons to the wall nuclei should exhibit the same dependence on position as the rf field coupling, namely, sech$x$. (Winter's wall-type excitations also lead to a factor sech$x$.) Including the factors $(1-r^2)h$, which also appear in the domain-wall description, does not give good agreement with the data. This indicates that the wave numbers k of the interacting magnons are large enough so that the corresponding wavelengths are small compared to the dimensions of the wall "membranes." This is reasonable since for spherical Fe particles, the maximum k values available are about 2×10^6 cm^{-1} corresponding to $\lambda\sim4\times10^{-6}$ cm, which is much smaller than the expected membrane radius ($\sim10^{-4}$ cm).

More precisely, the interaction between a nucleus and the magnetic electrons proceeds through the effective hyperfine coupling $A\mathbf{I}\cdot\mathbf{S}$, where A is defined to represent the interaction between the nuclear spin and the electronic spin system[6] and includes the position-dependent factor sech$x$. $\mathbf{I}$ and $\mathbf{S}$ are, respectively, the nuclear and electronic spin values. The relaxation rate due to single magnon emission or absorption is given by the well-known formula for transition rates

$$1/T_1(x) = (2\pi/\hbar)\langle I_f^z, n_k \pm 1 | A\mathbf{I}\cdot\mathbf{S} | I_i^z, n_k\rangle^2 \times \rho(\epsilon_k = \hbar\omega_0), \quad (3)$$

which is roughly evaluated in the Appendix. I_i^z and I_f^z are the initial and final nuclear-spin z components. Initially, we have n magnons of wave number $\mathbf{k}$. $\rho(\epsilon_k)$ is the spectral density of magnon modes of energy ϵ_k. The transition rate is proportional to n_k which, in the "high-temperature" approximation valid here, is proportional to temperature T giving rise to the observed linear temperature dependence. Thus from Eq. (3), we find that the relaxation rate $1/T_1 = (\text{sech}^2x)/T_{01}$[7] and is proportional to temperature, where T_{01} is the smallest relaxation time occurring at the center of the wall ($x=0$).

Indeed, we find that for pure Fe, the calculations of FID amplitude made with $T_1(x) = T_{01}/\text{sech}^2x$ give excellent agreement with the data at and below room temperature. Such calculated curves are shown as the solid lines in Figs. 1 and 3. In Fig. 1 note some of the distinctive shapes which are present in the data and reproduced in the calculations. Curves a and b correspond to conditions at which the nuclear magnetization at small t is larger than the equilibrium magnetization. Curve g shows a cusp which corresponds to a change in sign of the net x component of magnetization. We see that the shape of the decay curves is very dependent on the turning angles of the two pulses. The turning angles were varied by using a wide variety of combination of τ's and B_1's. For the data shown in Fig. 1, the τ's varied from about 1.2–12 μsec and the B_1's from about 0.5–5 G, while from the turning angles ranged from 2.3–16 rad. The results are fairly independent of the values of τ and B_1 as long as the turning angles are kept less than 16 rad (in agreement with the previous results[3]). In Fig. 3 we see that including the variation of T_1 with position in the wall gives a better fit to the data than can be obtained for any constant value of T_1. Thus, the *shape* of the curves indicates that the longitudinal relaxation takes place via emission or absorption of a single magnon.

The temperature dependence for pure Fe also supports this view. Figure 4 shows the relaxation rate

[6] H. Suhl, Phys. Rev. **109**, 606 (1958); J. Phys. Radium **20**, 333 (1959); T. Nakamura, Progr. Theoret. Phys. (Kyoto) **20**, 542 (1958).

[7] To be more precise we should write $1/T_1(x) = (\text{sech}^2x)/T_{01} + 1/T_d$, where T_d is the relaxation time of domain nuclei. However, in experiments designed to maximize the domain contribution (e.g., by going to very large turning angles where the domain-wall nuclei will tend to average out), we have never seen any evidence of the domain nuclei. This confirms that the overwhelming contribution to the observed signals come from nuclei in the wall, and we are justified in neglecting the second term.

at the center of the wall, $1/T_{01}$, as a function of temperature. We see that it is linear through room temperature, in agreement with Eqs. (3) and (A4). Table II lists the T_{01} values and maximum-enhancement factors at various temperatures for the two Fe samples. The errors are obtained from the spread in T_{01} values obtained by fitting the relaxation curves with a variety of turning angles combined with an estimate of the accuracy of the knowledge of the turning angles. For sample 1 we obtain a value of $1/T_{01}T=22\pm2$ sec^{-1} deg^1. The linear temperature dependence of the pure Fe sample indicates that the same regions and features of the magnon spectrum are available for magnon-nucleus interactions over this entire temperature range.

In the Appendix we roughly estimate the value of $1/T_{01}T$ resulting from the emission or absorption of bulk magnons assuming that they are not attenuated in the walls. There we also point out and discuss the fact that the usual dispersion relations used for a ferromagnet do not represent the ground state of real samples with nonuniform magnetization at zero applied field. Thus, since we do not have an expression for the real dispersion relation, it is impossible at this time to make a really reliable estimate of the relaxation rate. However, the rough estimates in the Appendix give $1/T_{01}T\sim5-700$ sec^{-1} deg^{-1}, so that it appears plausible that the demagnetizing fields do give rise to ample low-frequency magnons so that the absorption or emission of bulk magnons is the main mechanism of nuclear relaxation.

In order to see if we could observe any effects of a change in magnon spectrum with magnetic field, we measured T_1 in a field of about 2.7 kG at 4.2°K for sample 1. We observed no difference in T_1, but again obtained $T_{01}=11\pm2$ msec. This is to be expected, since in a sample with contiguous particles such as used in these experiments, the main initial effect due to applying an external field would probably be merely to shift the position of the domain walls. Therefore, until we get to high enough fields to sweep out the domain walls, we would expect T_1 and T_2 to remain unchanged; however, at these fields the domain wall signal has disappeared.

IV. TRANSVERSE RELAXATION IN PURE NATURAL Fe

The transverse relaxation time T_2 was obtained by measuring the echo height of a pair of pulses separated by a variable time t. Some T_2 relaxation curves of the echo heights as a function of the time between pulses are shown in Fig. 5. As was the case in the T_1 measurements, we find that the curves depend on the turning angles of the two pulses. The solid curves were calculated in a manner analogous to that used in the calculation of the T_1 curves. The x and y magnetization components are assumed to decay as $e^{-t/T_2(x)}$, where

$$1/T_2(x)=(\mathrm{sech}^2x)/T_{02}.$$

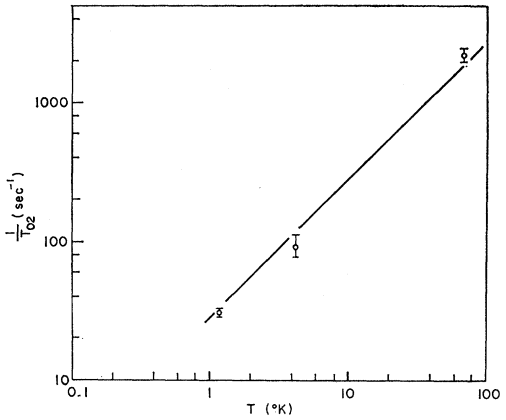

FIG. 6. Variation of transverse relaxation rate at the center of the wall as a function of temperature. The solid line corresponds to $1/T_{02}=28$ deg^{-1} sec^{-1}.

T_{02} is the smallest decay time at the center of the wall. (The transverse and longitudinal components are assumed to decay independently.) Using Eq. (21′) of Ref. 3 we thus obtain

$$\mathcal{E}(\omega_0,B_1,\tau_1,\tau_2)\sim\int_0^1\int_0^1\int_0^\infty\int_0^{\pi/2}\epsilon\,\sin\alpha_1\sin^2(\tfrac{1}{2}\alpha_2)\times e^{-t(\mathrm{sech}^2x)/T_{02}}p(h)r\,\sin\eta\,d\eta\,dx\,dr\,dh. \quad (4)$$

The solid curves shown in Fig. 5 are obtained by evaluating Eq. (4) on a computer. The shapes of the curves can be simply understood by considering the dependence on position of the enhancement factor and the relaxation time. We see that all the curves bend slightly upward with increasing time. This occurs because the nuclei have a spread in relaxation rates; the nuclei with faster relaxation rates decay out first leaving mainly the nuclei with slower relaxation rates at longer times. Also we see in Fig. 5 that the curves with smaller maximum turning angles fall more rapidly. This arises because at small turning angles we mainly observe nuclei with larger enhancement factors; these are nuclei near the center of the wall, which also have the fastest relaxation rates. As the turning angle becomes large the effects of the nuclei near the center of the wall tend to average out, and we mainly observe nuclei farther from the center of the wall, where the nuclei have slower relaxation rates. This is manifest by a relaxation curve of less slope.

From the usual simple argument that the magnons are transverse excitations and thus the longitudinal relaxation rate has matrix elements from both transverse components while the transverse rate has only one component available, we expect $1/T_2\geq1/2T_1$. This argument implies that the spectral density $\rho(\hbar\omega)$ of magnon modes is the same at both longitudinal ($\sim$46 Mc/sec) and transverse (0 Mc/sec) frequencies. Considering a possible difference in spectral densities and

TABLE III. Relaxation times at the center of the wall for enriched Fe and dilute Fe alloys.

Sample	T_{01} (msec)		T_{02} (msec)	
	1.2°K	4.2°K	1.2°K	4.2°K
90.7% Fe^{57}	125±10	60±5	~11	~9
1 *a/o* Co	550±50	170±20	31±4	23±2
3.8 *a/o* Al	1000±200	500±100	33±2	20±2

that other relaxation processes may occur, we write

$$1/T_2=[\rho(0)/\rho(\hbar\omega_0)](1/2T_1)+1/T_2', \qquad (5)$$

where $1/T_2'$ is due to mechanisms other than single-magnon emission or absorption. Another relaxation mechanism we might expect to be present is that of spin-spin interactions of the Suhl-Nakamura (SN) type.[6] This interaction [due to spin flips by emission (absorption) of a virtual magnon by one nucleus and subsequent reabsorption (emission) by a second nucleus] is expected to be temperature-independent since it involves virtual magnons. However, over the temperature range 1.2–78°K we find a linear temperature dependence as shown in Fig. 6. The measured values of the relaxation times at the center of the wall for sample 1 are listed in column 3 of Table II. We obtain a value of $1/T_{02}T=28\pm3$ sec^{-1} deg^{-1} for sample 1. Thus, there appears to be no contribution from a SN type interaction in Fe with the natural abundance of Fe^{57}.

The data are fitted well by the relation $1/T_2=2.5/2T_1$. As mentioned, if the magnons were purely transverse (or, equivalently, if the spin susceptibility in the direction of magnetization were equal to 0), we would expect $1/T_2=1/2T_1$. For isotropic magnons we would have $1/T_2=1/T_1$. Thus we expect the ratio of T_1/T_2 to be between $\frac{1}{2}$ and 1 (closer to $\frac{1}{2}$ for Fe), depending on the degree of anisotropy of the spin susceptibility. The simplest interpretation of the factor 2.5 is that $\rho(0)/\rho(\hbar\omega_0)\sim2.5$. This is a rather unusual result, but as we noted earlier we do not know the true form of the dispersion relation, so it is difficult to ascertain whether it is reasonable.

V. RELAXATION RATES IN ENRICHED Fe AND SOME DILUTE Fe ALLOYS; SEARCH FOR SN INTERACTION

In order to look for the SN interaction we also measured the T_1 and T_2 values of 90.7% enriched Fe^{57} sample at 1.2 and 4.2°K. Unfortunately, the enriched Fe^{57} sample behaved as if it were quite impure. It had a FID time of about one-half that of pure Fe corresponding to a frequency spectrum width of about twice that of pure Fe. The longitudinal relaxation curves were well behaved, i.e., they varied with turning angle in the expected manner. The values obtained for the center of the domain wall T_{01} are listed in Table III. However, the transverse relaxation curves did not behave in a manner typical of the natural Fe samples: They were independent of turning angle and rf field, and had an increasing slope at longer times, as if some mechanism other than single emission of absorption of a magnon were causing the relaxation. Some of these features have also been seen in dilute alloys of Fe containing 1–3 at.% solute atoms. T_{01} and T_{02} for some alloys are also listed in Table III. As can be seen from Tables II and III, at a given temperature the observed T_{01} values for the dilute alloys are much longer than the T_{01} value for pure Fe, the differences being greater the less pure the sample. We speculate that these increases in the T_1 relaxation times are due to two possible effects: The impurities lead to localized magnon states which change the magnon spectrum in such a way that less magnons are available for the relaxation process; the impurities reduce the coupling between the magnon states and the nuclei, thereby causing longer relaxation times. The T_{02} relaxation times in the alloys are considerally less than the T_{01} relaxation times and of comparable values to those in pure Fe. They are also tabulated in Table III. The smaller relaxation times (or larger T_2 relaxation rates) are reasonable, since it seems likely that there is an added T_2 relaxation mechanism present in these sample. The impurities tend to act like pinning points for the domain walls; in general, this decreases the enhancement factor as observed for the dilute alloys (see Ref. 3) and also leads to considerable variation in the total energy of the sample depending on the domain-wall position. Thus, in the impure samples it becomes quite probable that the wall may not return to the same position after each rf pulse. This can lead to each domain-wall nucleus being in a slightly different magnetic field after each pulse which would give an apparent added contribution to the T_2 relaxation mechanism. (This mechanism causes doubt about the reliability of T_2 measurements made by applying a dc magnetic field some time within the T_2 measuring sequence. If, as is likely, the domain wall returns to a different position after the dc field is turned off, there may be an apparent added contribution to the T_2 decay rate due to this mechanism.) Because of this added pseudorelaxation process, we are unable to ascertain with certainty how much of the measured T_2 relaxation rate is due to the SN interaction. However, we can estimate an upper limit as follows: Since the natural Fe alloys have 40 times less Fe^{57} than the enriched sample, we assume that the T_{02} relaxation rates of the alloys give a measure of all relaxation processes other than the SN interaction. At the lowest temperature, where the SN mechanism should be most evident, these processes give a contribution to the T_{02} rate of about 30 sec^{-1}. The total T_{02} rate for the enriched Fe, which is assumed to decay by the same processes as the alloys plus a SN interaction, is about 100 sec^{-1}. Thus, an upper limit for the SN interaction is about 70 sec^{-1} for the 90.7% Fe^{57} sample. Within the approximation of the Van Vleck moment formula (as used in the SN rate calculation),[6] we expect the SN interaction rate to be proportional to the Fe^{57} concentration. Thus, assuming a SN rate of about 80

TABLE IV. Values of parameters of Fe.

$\hbar\omega_0$	3.1×10^{-19} erg
$\hbar\omega_m$	4×10^{-16} erg
$\hbar\omega_{ex}(=2JS)$	5.6×10^{-14} erg
$D(=2JSa^2)$	4.6×10^{-29} erg cm^2
$A_0/\hbar$ $(A_0\mathbf{I}\cdot\mathbf{S}=\mu H_{int})$	2.9×10^{8} rad sec^{-1}
a	2.86×10^{-8} cm
S	1

sec^{-1} for 100% Fe^{57}, for natural Fe we would expect a SN contribution of about 2.5 sec^{-1}, which would be unobservable at 1.2°K, where the T_{02} relaxation rate is measured to be 30 ± 2 sec^{-1}. This is consistent with the previous conclusion that we see no SN-type contribution in the natural Fe samples.

Unfortunately we are not able to obtain a really valid estimate of the SN interaction rate from the formulas derived by Suhl and Nakamura. In Ref. 6 they used the Van Vleck moment formula to obtain the broadening due to their interaction. However, for the present case, the Van Vleck (VV) formula is invalid since here we excite both species of spin by the rf pulse whereas the VV formula is derived for the case where the two spin species are well separated in frequency so, that only one is excited by the rf pulse. However, if, for the sake of comparison, we ignore this difficulty and use the SN formula to estimate the SN interaction rate, we have

$$\frac{1}{T_{SN}}\simeq\langle\Delta\nu^2\rangle^{1/2}\simeq\frac{1}{2\pi}\left(\frac{I(I+1)}{24\pi}\right)^{1/2}\left(\frac{\omega_{ex}}{\omega_H}\right)^{1/4}\frac{A^2S}{\hbar^2\omega_{ex}}, \quad (6)$$

where it was assumed that the dispersion relation is $\epsilon_k=\hbar(\omega_H+\omega_{ex}a^2k^2)$ and ω_H has been taken as $2\pi\gamma M_s$ (assuming the demagnetizing factor is $\frac{1}{2}$). All other quantities have been previously defined and the parameters used to evaluate Eq. (6) are listed in Table IV. From Eq. (6) we estimate $1/T_{SN}\sim60$ sec^{-1}, which is in acceptable agreement with the upper limit of about 80 sec^{-1} for a 100% Fe^{57} sample. Thus it appears reasonable that at 1.2 and 4.2°K, the major portion of the T_2 relaxation mechanism in the enriched Fe sample is due to spin-spin interactions of the SN type. It has been claimed[1,2,8] that the observed T_2 relaxation in enriched Ni(94% Ni^{61}) and Co^{59} samples was due to the SN interaction. Using the upper limit for the SN interaction obtained here for Fe, we can estimate the values for Co and Ni and compare these with the measured values (which may be quite inaccurate since the variation of ϵ and $1/T_2$ with position in the wall was not considered). We shall assume that Eq. (6) at least represents the factors envolved in the SN interaction, and scale the parameters properly for Co and Ni. Using $(A/\hbar)_{Co}=1.4\times10^9$ rad sec^{-1}, M_s(Co)=1.4 kG, $I_{Co}=\frac{7}{2}$, and $\omega_{ex}(Co)\approx\omega_{ex}(Fe)(1400°K/1040°K)$, we obtain $1/T_{SN}(Co)\sim7000$ sec^{-1}. Weger[2] gives $1/T_2$(Co) at 11°K to be $(10\text{–}30)\times10^3$ sec^{-1}. Consequently, at this temperature it appears reasonable that at least some of the observed T_2 relaxation might be due to the SN interaction. For Ni, using $(A/\hbar)_{Ni}=2.7\times10^8$ rad sec^{-1}, M_s(Ni)=0.5 kG, $I_{Ni}=\frac{3}{2}$, and $\omega_{ex}(Ni)\approx0.6\omega_{ex}(Fe)\times630/1040$, we obtain $1/T_{SN}(Ni)\sim400$ sec^{-1}. Weger measured $1/T_2\simeq3000$ sec^{-1} at 11°K for a 94% Ni^{61} sample. This appears to be too high a value for the SN interaction and is more likely mainly due to other processes discussed earlier.

[8] A. M. Portis and A. C. Gossard, J. Appl. Phys. **31**, 205S (1960).

VI. CONCLUSIONS

We find that in pure natural Fe the relaxation rates of nuclei in the domain wall vary with position in the wall as $(\mathrm{sech}^2x)/T_0$, where x is the distance from the center of the wall. Independently, from *both* the shapes and the temperature dependence of the relaxation curves we find that the predominate relaxation mechanism for both the longitudinal and transverse relaxation is due to the single emission or absorption of real magnons. These are most likely bulk magnons, characteristic of the domains. For the longitudinal relaxation rate we measure $1/T_{01}T=22\pm2$ sec^{-1} deg^{-1}, where $1/T_{01}$ is the fastest decay rate at the center of the wall. For the transverse rate we measure $1/T_{02}T=28\pm3$ sec^{-1} deg^{-1}.

In a sample of Fe enriched to 90.7% Fe^{57} we also observe another relaxation mechanism at low temperatures. We attribute this mainly to a spin-spin interaction of the SN type.

ACKNOWLEDGMENTS

The author is indebted to Dr. A. W. Overhauser and Dr. A. D. Brailsford for many helpful discussions and suggestions.

APPENDIX: ESTIMATE OF LONGITUDINAL RELAXATION RATE

As discussed in the text, let us assume that the main mode of interaction is with the bulk magnons and that they have their full amplitude in the wall. We thus attempt to estimate the relaxation rate in the domains and equate this to the value at the center of the wall.

Since Fe^{57} has a nuclear spin $\frac{1}{2}$, for a single-magnon emission or absorption we have[9]

$$\frac{1}{T_1}=2\frac{2\pi}{\hbar}\sum_k\langle f|\mathcal{H}|i\rangle^2\ \delta(E_i-E_f), \quad (A1)$$

where i and f are the initial and final states of the electronic-nuclear spin system and $\mathcal{H}$ is the interaction

[9] The following treatment is given many places; we closely follow the notation used by D. Beeman and P. Pincus, Phys. Rev. **166**, 359 (1968).

inducing the transition. For magnon creation we have

$$\mathcal{H}=\tfrac{1}{2}AI^{+}\left(\frac{2S}{N}\right)^{1/2}\sum_k b_k^{\dagger}, \tag{A2}$$

where I^+ is the raising operator for the nuclear spin, N is the number of atomic spins in the solid and $b_k^\dagger$ is the boson operator for creation of spin waves of wave vector $\mathbf{k}$. Letting $A=A_0\,\mathrm{sech}x$ and $1/T_1=(\mathrm{sech}^2x)/T_{01}$, we obtain

$$\frac{1}{T_{01}}=\frac{2\pi}{\hbar}A_0^2\frac{S}{N}\sum_k\left[n_k(n_k+1)\right]^{1/2}\delta(\epsilon_k-\hbar\omega_0). \tag{A3}$$

In the high-temperature limit, $[n_k(n_k+1)]^{1/2}\sim k_BT/\hbar\omega_0$. Substituting in this value and writing $\sum_k\delta(\epsilon_k-\hbar\omega_0)$ in terms of the spectral density function $\rho(k)$, we obtain

$$\frac{1}{T_0}=\frac{2\pi}{\hbar}\frac{A_0^2S}{N}\frac{k_BT}{\hbar\omega_0}\int_0^{k_{\max}}\rho(k)dk. \tag{A4}$$

The whole problem of evaluating Eq. (A4) then becomes that of knowing $\rho(k)$ or the magnon dispersion relation from which $\rho(k)$ can be derived. The dispersion relations usually given for ferromagnets are clearly incorrect at zero applied field. For example, the usual approximate dispersion relation,

$$\epsilon_k=Dk^2+\hbar\omega_i+\tfrac{1}{2}\hbar\omega_m\sin^2\theta_k, \tag{A5}$$

gives some negative values of ϵ_k for most shapes of particles. [All the quantities have the usual notation[10], $\omega_i=\gamma(H_0-4\pi N_zM_s)$ and $\omega_m=4\pi\gamma M_s$, where H_0 is the applied field, N_z is the demagnetization factor in the z direction, and M_s is the saturation magnetization. θ_k is the angle between the domain magnetization and the direction of propagation of the magnon of wave vector $\mathbf{k}$.] These are, therefore, unstable states, and thus Eq. (A5) does not represent the ground state of a ferromagnet material of finite size in zero external field where we have a nonuniform magnetization. The usual exact dispersion relation,

$$\epsilon_k=\left[(Dk^2+\hbar\omega_i)(Dk^2+\hbar\omega_i+\hbar\omega_m\sin^2\theta_k)\right]^{1/2}, \tag{A6}$$

gives both negative and imaginary values for the energies when $H_0=0$. Thus, it also does not represent the ground state of real ferromagnets which have a domain structure. Since a longitudinal relaxation process conserves energy, the magnons will have a fixed energy $\epsilon_k=\hbar\omega_0$; it is just the manifold nature of the dispersion relation which allows many k values for a given ϵ_k, and thus the integral over $\rho(k)$ may become quite large. Since $\omega_m\sim1000\omega_0$, we are interested in ϵ_k very near zero. Here the above dispersion relations are especially poor in representing the true dispersion relations. Nevertheless, in order to get a very rough estimate of the value of $1/T_{01}$, let us use Eq. (A5) for a spherical domain. Then $\omega_i=-\frac{1}{3}\omega_m$ and $Dk_{\max}{}^2\simeq\frac{1}{3}\hbar\omega_m$. The spectral density function for this approximate dispersion relation is[10]

$$\rho(k)=Vk^2/2\pi^2\hbar\omega_m\cos\theta_k. \tag{A7}$$

Evaluating $\int_0^{k_{\max}}\rho(k)dk$ over a path of constant $\epsilon_k(=\hbar\omega_0)$ and putting this into Eq. (A4) we get $1/T_{01}T\sim700$ sec^{-1} deg^{-1}. An evaluation using the dispersion relation given in Eq. (A6) with its corresponding spectral density function

$$\rho(k)=\frac{Vk^2}{2\pi^2\hbar\omega_m\cos\theta_k}\frac{\hbar\omega_k}{Dk^2+\hbar\omega_i}, \tag{A8}$$

gives $1/T_{01}T\sim5$ sec^{-1} deg^{-1}. The parameters for Fe used in this estimate are given in Table IV. Again let us emphasize that the value of $\int_0^{k_{\max}}\rho(k)dk$ depends very strongly on the form of the dispersion relation near $\epsilon_k=0$, and since we do not know the true behavior of ϵ_k we can say little about the reliability of the above estimates. However, the estimate indicates that it seems reasonable that due to the demagnetizing fields, there are ample magnons available at $\epsilon_k=\hbar\omega_0$ to cause the observed nuclear relaxation rates.

[10] M. Sparks, *Ferromagnetic Relaxation Theory* (McGraw-Hill Book Co., New York, 1964).